Dither Signal Design for PAPR Reduction in OFDM-IM

Shinya Watanabe* Teruyuki Miyajima* Yoshiki Sugitani*
*Graduate School of Science and Engineering, Ibaraki University, Japan

***Abstract*—This paper proposes a peak-to-average power ratio (PAPR) reduction method using a time-domain dither signal for orthogonal frequency division multiplexing with index modulation (OFDM-IM) systems. The dither signal is determined so as not only to reduce PAPR at the transmitter but also to avoid the misdetection of active subcarriers at the receiver. Unlike conventional methods, we make use of the channel knowledge at the transmitter to keep the dither signal components in the DFT output at the receiver sufficiently low. Simulation results show that the proposed method is significantly superior to a conventional method in terms of bit error rate performance while preserving similar PAPR performance.**

I. Introduction

Orthogonal frequency division multiplexing with index modulation (OFDM-IM) is a new multi-carrier modulation scheme, where the concept of the index modulation of spatial modulation is applied to the subcarriers of OFDM systems [1], [2], [3]. In OFDM-IM, a subset of subcarriers are selected as active subcarriers, and the remaining subcarriers are unused for data transmission. Unlike conventional OFDM, the information bits are conveyed by not only modulating the active subcarriers but also selecting the active subcarriers. OFDM-IM provides a trade-off between error performance and spectral efficiency and is a possible candidate for high-speed wireless communications and machine-to-machine communications.

It was shown in [4] that OFDM-IM suffers from high peak-to-average power ratio (PAPR) as well as the conventional OFDM. When a transmit signal passes through a nonlinear high power amplifier, high PAPR causes the deterioration of BER and undesired out-of-band radiation due to nonlinear distortion. So far, various PAPR reduction techniques have been proposed for OFDM systems [5]. Although these methods could be applied to reduce the PAPR of OFDM-IM transmit signals, they might not be efficient because they do not take the inherent characteristics of the OFDM-IM signals into consideration.

There have been PAPR reduction methods intended for OFDM-IM systems [6], [7], [8]. In [6], a frequency-domain dither signal to reduce PAPR is inserted into inactive subcarriers which are unused for data transmission. A crucial task at the receiver of OFDM-IM is to detect the active subcarriers. To avoid the misdetection of the active subcarriers, the magnitude of the dither signal in frequency-domain is limited to a predetermined level. Clearly, the magnitude limitation level has a tradeoff between the PAPR reduction and the misdetection performance. Therefore, this method is not suitable for higher-order QAM since the minimum magnitude of QAM symbols is small, and thus, the magnitude limitation level cannot be large. To overcome the disadvantage of the single-level dither signal in [6], multilevel frequency-domain dither signals are employed in [7]. The dither signals are determined so as to reduce the misdetection by taking into consideration the characteristics of the transmit signal. However, this method does not consider the channel characteristics despite that the active subcarrier detection is affected by the channel. Also, in [6], [7], the maximum likelihood detector, whose complexity can be prohibitively high, is used for the detection of active subcarriers and data symbols. In [8], a low-complexity PAPR reduction method was proposed. Dither signals corresponding to inactive subcarriers are generated by clipping the time-domain transmit signal. Although PAPR can be effectively reduced, this method suffers from BER degradation because the magnitude of the dither signal is not strictly limited. Also, in [8], the combination of the dither signal and active constellation extension (ACE) was proposed, however, the effectiveness of the ACE is very limited.

In this paper, we propose a time-domain dither signal design method to reduce PAPR of OFDM-IM signals. In the proposed method, to avoid the active subcarrier misdetection, the dither signal components in the DFT outputs at the receiver are sufficiently kept low by making use of the knowledge of the channel. To the best of our knowledge, this is the first attempt to investigate a dither signal design using the channel knowledge at the transmitter of OFDM-IM. The advantages of the proposed method are two-fold: 1) the proposed method can reduce PAPR at the transmitter without sacrificing BER by reducing the misdetection of active subcarriers at the receiver, and 2) the properly designed dither signals enable the use of a low-complexity energy-based detector [9].

The rest of the paper is organized as follows. In Section II, the system model of the proposed method is introduced. In Section III, a dither signal design is proposed. Then, computer simulation results are provided in Section IV. Finally, the paper is concluded in Section V.

The following notations are used. $C(n,k)$ denotes the binomial coefficient. $\lfloor \cdot \rfloor$ denotes the maximum integer no larger than the argument. $\| \cdot \|_2$ and $\| \cdot \|_\infty$ denote the 2-norm and the infinity norm of a vector, respectively. $\mathbf{I}_N$ denotes $N \times N$ identity matrix. $\mathbf{0}_N$ denotes $N \times 1$ zero vector. $\mathbf{1}$ denotes the vector of all ones. $(\cdot)^T$ and $(\cdot)^H$ denote transpose and conjugate transpose, respectively. $\mathbb{R}$ and $\mathbb{C}$ denote real and complex number fields, respectively. $\mathrm{E}[\cdot]$ denotes the expectation operator. $\mathrm{diag}(\mathbf{a})$ represents a diagonal matrix whose diagonal entries consist of the entries of vector $\mathbf{a}$.

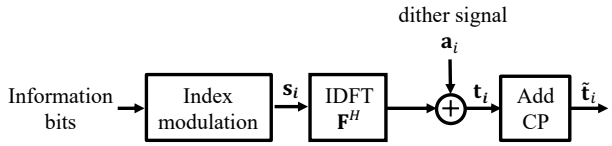

Fig. 1. Transmitter structure.

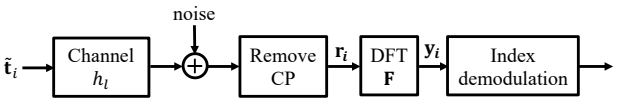

Fig. 2. Receiver structure.

II. System Model

A. Transmitter

Figure 1 shows the transmitter structure of the proposed system. In OFDM-IM systems, m information bits are divided into g sub-blocks containing p bits, and N subcarriers are divided into g sub-blocks, each with n subcarriers, i.e., $m = pg$ and $N = ng$. In each sub-blocks, only k out of n subcarriers are employed for data transmission, which are called active subcarriers. The remaining $n-k$ subcarriers are not employed for data transmission, which are called inactive subcarriers. Also, p bits are divided into p_1 bits and p_2 bits, where $p_1 = \lfloor \log_2(C(n,k)) \rfloor$ bits are called index bits and $p_2 = k\log_2(M)$ bits are called symbol bits. The number of combinations of active subcarriers is $c = 2^{p_1}$. We represent the jth combination as $\mathcal{X}_j = \{l_{j,0}, \cdots, l_{j,k-1}\}$ where $l_{j,q} \in \{0, \cdots, n-1\}$ is the index of the qth active subcarrier. A set of all combinations is denoted by $\mathcal{Y} = \{\mathcal{X}_0, \cdots, \mathcal{X}_{c-1}\}$. In each sub-blocks, the combination of k active subcarriers corresponding to p_1 index bits is chosen from $\mathcal{Y}$ based on a look-up table, and then p_2 symbol bits are mapped onto data symbols $\{d_i\}$ that modulate the active subcarriers.

Concatenating g modulated sub-blocks, the ith OFDM-IM frequency domain data block of length N is represented as

$$\mathbf{s}_i = \begin{bmatrix} s_{iN} & s_{iN+1} & \cdots & s_{(i+1)N-1} \end{bmatrix}^T = \mathbf{M}_i \mathbf{d}_i \tag{1}$$

where an $N \times K$ matrix $\mathbf{M}_i$ consists of K columns of $\mathbf{I}_N$ and each column corresponds to active subcarriers, $\mathbf{d}_i = [d_{iK} \ \cdots \ d_{(i+1)K-1}]^T$ is the data symbol vector whose element is a QAM symbol, and $K = kg$ is the total number of active subcarriers. Then, s_j is a QAM symbol if the jth subcarrier is active and 0 otherwise. By taking the inverse discrete Fourier transform (IDFT) of $\mathbf{s}_i$, we obtain a time-domain OFDM-IM signal. To suppress PAPR of the transmit signal, we add a time-domain dither signal $\mathbf{a}_i$ to the OFDM-IM signal as

$$\mathbf{t}_i = \begin{bmatrix} t_{iN} & \cdots & t_{(i+1)N-1} \end{bmatrix}^T = \frac{1}{\sqrt{K}} \mathbf{F}^H \mathbf{s}_i + \mathbf{a}_i \tag{2}$$

where $\mathbf{F}$ denotes the N-point DFT matrix whose (j_1, j_2)th element is $\exp(-j2\pi(j_1-1)(j_2-1)/N)$. The dither signal $\mathbf{a}_i$ is given by $\mathbf{a}_i = \mathbf{P}_i \mathbf{u}_i$ where $\mathbf{P}_i$ is an $N \times (N-K)$ orthonormal precoding matrix and $\mathbf{u}_i$ is a PAPR reduction vector of length $N-K$. The normalization factor of $1/\sqrt{K}$ is used to ensure the same average transmission energy with conventional OFDM. Our purpose is to determine $\mathbf{P}_i$ and $\mathbf{u}_i$ to suppress PAPR of the OFDM-IM transmit signal without sacrificing error performance.

After a cyclic prefix (CP) of length N_p is added to $\mathbf{t}_i$, a time-domain signal $\tilde{\mathbf{t}}_i$ of length $Q = N + N_p$ is obtained as $\tilde{\mathbf{t}}_i = [\tilde{t}_{iQ} \ \cdots \ \tilde{t}_{(i+1)Q-1}]^T = [t_{(i+1)N-N_p} \ \cdots \ t_{(i+1)N-1} \ t_{iN} \ \cdots \ t_{(i+1)N-1}]^T$.

Finally, the signal $\tilde{t}_j$ is transmitted over a frequency-selective Rayleigh fading channel after power amplification.

B. Receiver

Fig. 2 shows the receiver structure. The received signal is given by

$$r_j = \sum_{l=0}^{L_h} h_l \tilde{t}_{j-l} + n_j \tag{3}$$

where h_l is the impulse response of the channel of order L_h and n_j is an additive white Gaussian noise. We assume that $L_h \le N_p$ to avoid inter-block interference. After CP removal, the received signal vector of length N is represented as

$$\begin{aligned} \mathbf{r}_i &= \begin{bmatrix} r_{iQ+N_p} & r_{iQ+N_p+1} & \cdots & r_{(i+1)Q-1} \end{bmatrix}^T \\ &= \mathbf{H}_c \mathbf{t}_i + \mathbf{n}_i \\ &= \frac{1}{\sqrt{K}} \mathbf{H}_c \mathbf{F}^H \mathbf{s}_i + \mathbf{H}_c \mathbf{a}_i + \mathbf{n}_i \end{aligned} \tag{4}$$

where $\mathbf{n}_i = [n_{iQ+N_p} \ \cdots \ n_{(i+1)Q-1}]^T$ and $\mathbf{H}_c$ is an $N \times N$ circulant channel matrix given by

$$\mathbf{H}_c = \begin{bmatrix} h_0 & 0 & 0 & h_{L_h} & \cdots & h_1 \\ h_1 & h_0 & \ddots & \ddots & \ddots & \vdots \\ \vdots & & \ddots & \ddots & \ddots & h_{L_h} \\ h_{L_h} & & & \ddots & \ddots & 0 \\ & \ddots & & & \ddots & 0 \\ 0 & & h_{L_h} & \cdots & \cdots & h_0 \end{bmatrix}.$$

After applying DFT to $\mathbf{r}_i$, the frequency domain received signal $\mathbf{y}_i$ can be represented as

$$\begin{aligned} \mathbf{y}_i &= \begin{bmatrix} y_{i,0} & y_{i,1} & \cdots & y_{i,N-1} \end{bmatrix}^T \\ &= \frac{\sqrt{K}}{N} \mathbf{F} \mathbf{r}_i \\ &= \frac{1}{N} \mathbf{F} \mathbf{H}_c \mathbf{F}^H \mathbf{s}_i + \frac{\sqrt{K}}{N} \mathbf{F} \mathbf{H}_c \mathbf{a}_i + \mathbf{z}_i \end{aligned} \tag{5}$$

where $(\mathbf{F}\mathbf{H}_c\mathbf{F}^H)/N$ becomes diagonal matrix whose diagonal entries are samples of the channel transfer function and $\mathbf{z}_i = (\sqrt{K}\mathbf{F}\mathbf{n}_i)/N$.

Finally, we detect the information bits from $\mathbf{y}_i$. Maximum likelihood detection is often employed [3], but its complexity

is prohibitively high. Here, we consider a low-complexity energy-based detection scheme [9], where first the active subcarriers are detected, then their corresponding data symbols are detected. Since the active subcarrier detection is performed for each sub-blocks, we denote the γth sub-block of $\mathbf{y}_i$ in (5) as $\mathbf{y}_i^{(\gamma)} = [y_{i,\gamma n} \ \cdots \ y_{i,(\gamma+1)n-1}]^T$. The detection process is summarized below.

Step1) Detect the index bits for γth sub-block:

1) Compute the signal energy $|y_{i,\zeta}|^2$ for $\gamma n \le \zeta \le (\gamma+1)n-1$ and arrange in descending order.
$$|y_{i,\zeta_0}|^2 \ge |y_{i,\zeta_1}|^2 \ge \cdots \ge |y_{i,\zeta_{n-1}}|^2 \tag{6}$$
where ζ_j is the index of the jth largest energy subcarrier.
2) Detect the active subcarriers iteratively. Let $\mathcal{Y}_0 = \mathcal{Y}$. Construct $\mathcal{Y}_1$ consisting of $\mathcal{X}_j$s where $\mathcal{X}_j$ is included in $\mathcal{Y}_0$ and contains ζ_0. If $\mathcal{X}_j$ containing ζ_0 does not exist in $\mathcal{Y}_0$, find $\mathcal{X}_j$ containing the next largest subcarriers ζ_1, and so on. Repeat this process k times, finally there is one $\mathcal{X}_j$ in $\mathcal{Y}_k$. Let the elements of $\mathcal{X}_j$ in $\mathcal{Y}_k$ be active subcarrier indices.
3) Find the index bits corresponding to the active subcarriers based on the look-up table.

Step2) Detect the symbol bits. Construct a matrix $\hat{\mathbf{M}}_i$ which has K columns of $\mathbf{I}_N$ and each column corresponds to the active subcarriers detected by Step1-2). By multiplying $\hat{\mathbf{M}}_i^H$ with $\mathbf{y}_i$ in (5), we obtain
$$\begin{aligned}\hat{\mathbf{y}}_i &= \hat{\mathbf{M}}_i^H \mathbf{y}_i \\ &= \mathbf{\Omega}_i \mathbf{d}_i + \frac{\sqrt{K}}{N}\hat{\mathbf{M}}_i^H \mathbf{F}\mathbf{H}_c\mathbf{a}_i + \hat{\mathbf{M}}_i^H \mathbf{z}_i, \end{aligned} \tag{7}$$
where $\mathbf{\Omega}_i = (\hat{\mathbf{M}}_i^H \mathbf{F}\mathbf{H}_c\mathbf{F}^H\mathbf{M}_i)/N$. We perform zero-forcing frequency-domain equalization as $\hat{\mathbf{d}}_i = \mathbf{\Omega}_i^{-1}\hat{\mathbf{y}}_i$ and obtain the symbol bits from the decision of $\hat{\mathbf{d}}_i$.

In the energy-based scheme, if the active subcarrier detection is failed, the error performance seriously degrades. Thus, it is crucial to design the dither signal $\mathbf{a}_i$ such that it does not affect the active subcarrier detection.

III. PAPR REDUCTION USING DITHER SIGNAL

A. Dither signal design

First, we determine the precoding matrix $\mathbf{P}_i \in \mathbb{C}^{N\times(N-K)}$. In the DFT output at the receiver, there exists interference due to the dither signal, which corresponds to the second term in (7). To suppress the interference, we borrow the idea presented in [10], which was originally developed for OFDM systems. By assuming that the perfect channel state information (CSI) is available at the transmitter, we can determine $\mathbf{P}_i$ so that the interference in the DFT outputs corresponding to the active subcarriers is zero. Specifically, $\mathbf{P}_i$ is chosen so as to satisfy the following conditions.
$$\begin{cases} \mathbf{M}_i^H \mathbf{F}\mathbf{H}_c\mathbf{P}_i = \mathbf{0}_K \\ \mathbf{P}_i^H\mathbf{P}_i = \mathbf{I}_{N-K} \end{cases}. \tag{8}$$

From (8), $\mathbf{P}_i$ belongs to the null space of $\mathbf{\Gamma}_i = \mathbf{M}_i^H\mathbf{F}\mathbf{H}_c \in \mathbb{C}^{K\times N}$. Using the singular value decomposition, $\mathbf{\Gamma}_i$ can be decomposed as $\mathbf{\Gamma}_i = \mathbf{U}_i\mathbf{\Sigma}_i\mathbf{V}_i^H$, where $\mathbf{U}_i \in \mathbb{C}^{K\times K}$ and $\mathbf{V}_i \in \mathbb{C}^{N\times N}$ are unitary matrices consisting of the singular vectors of $\mathbf{\Gamma}_i$, and $\mathbf{\Sigma}_i \in \mathbb{R}^{K\times N}$ is a matrix containing the singular values of $\mathbf{\Gamma}_i$. Since the null space of $\mathbf{\Gamma}_i$ is spanned by the last K columns of $\mathbf{V}_i = [\mathbf{v}_{i,0}, \mathbf{v}_{i,1}, \ldots, \mathbf{v}_{i,N-1}]$, the precoding matrix $\mathbf{P}_i$ can be formed by
$$\mathbf{P}_i = \begin{bmatrix} \mathbf{v}_{i,N-K} & \mathbf{v}_{i,N-K+1} & \cdots & \mathbf{v}_{i,N-1} \end{bmatrix}. \tag{9}$$

Next, we determine the PAPR reduction vector $\mathbf{u}_i$. We evaluate the PAPR of the transmitted signal defined by
$$\mathrm{PAPR} = \frac{\|\hat{\mathbf{t}}_i\|_\infty^2}{\mathrm{E}[\|\hat{\mathbf{t}}_i\|_2^2]} \tag{10}$$
where $\hat{\mathbf{t}}_i$ is the oversampled transmit signal. From (2), we have $\hat{\mathbf{t}}_i = (\mathbf{F}_{F_s}^H(\mathbf{s}_i + \mathbf{F}\mathbf{P}_i\mathbf{u}_i))/\sqrt{K}$, where $\mathbf{F}_{F_s} \in \mathbb{C}^{N\times F_sN}$ is the oversampled DFT matrix with the oversampling factor F_s. To reduce PAPR, we minimize the numerator of (10). Given the precoding matrix $\mathbf{P}_i$, the PAPR reduction vector $\mathbf{u}_i$ is determined by solving the following constrained optimization problem.
$$\begin{aligned} \min_{\mathbf{u}_i} \ & \left\| \frac{1}{\sqrt{K}}\mathbf{F}_{F_s}^H(\mathbf{s}_i + \mathbf{F}\mathbf{P}_i\mathbf{u}_i) \right\|_\infty \\ \text{subject to} \ & \left\| \frac{\sqrt{K}}{N}\mathbf{F}\mathbf{H}_c\mathbf{P}_i\mathbf{u}_i \right\|_\infty \le \beta\sigma H_{\min}, \\ & \left\| \frac{1}{\sqrt{K}}\mathbf{F}_{F_s}^H\mathbf{F}\mathbf{P}_i\mathbf{u}_i \right\|_2 \le \sqrt{\alpha}\left\|\breve{\mathbf{t}}_i\right\|_2 \end{aligned} \tag{11}$$
where σ is the minimum amplitude of the transmit symbols, $H_{\min} = \min|\mathrm{diag}\{(\mathbf{F}\mathbf{H}_c\mathbf{F}^H)/N\}|$ is the minimum magnitude of the channel transfer function, $\breve{\mathbf{t}}_i = (\mathbf{F}_{F_s}^H\mathbf{s}_i)/\sqrt{K}$ corresponds to the data component in the transmit signal, and α and β are parameters to control the effect of the constraints.

In (11), the first constraint ensures that the maximum value of the interference due to the dither signal is sufficiently smaller than the minimum value of the data components in the DFT output. As a result, we can expect to avoid the failure of active subcarriers detection. The second constraint suppresses the power of the dither signal compared to the power of the data component in the transmit signal. Due to these constraints, we can expect that error performance degradation is noticeably alleviated. Note that the objective function and the constraints in (11) are convex.

B. Solving optimization problem

To obtain a solution of (11), we reformulate the optimization problem. First, we rewrite the problem (11) as
$$\begin{aligned} \min_{\mathbf{u}_i} \ & \left\| \breve{\mathbf{t}}_i + \breve{\mathbf{P}}_i\mathbf{u}_i \right\|_\infty \\ \text{subject to} \ & \left\| \breve{\mathbf{Q}}_i\mathbf{u}_i \right\|_\infty \le \beta_1, \ \left\| \breve{\mathbf{P}}_i\mathbf{u}_i \right\|_2 \le \sqrt{\alpha}\left\|\breve{\mathbf{t}}_i\right\|_2 \end{aligned} \tag{12}$$

where $\breve{\mathbf{Q}}_i = (\sqrt{K}\mathbf{F}\mathbf{H}_c\mathbf{P}_i)/N$, $\beta_1 = \beta\sigma H_{\min}$, and $\breve{\mathbf{P}}_i = (\mathbf{F}_{Fs}^H\mathbf{F}\mathbf{P}_i)/\sqrt{K}$. Next, we convert the problem (12) to the real-valued form with real variables defined as follows:

$$\begin{aligned}
\breve{\mathbf{t}}_i^R &= \left[\mathrm{Re}\{\breve{\mathbf{t}}_i^T\} \quad \mathrm{Im}\{\breve{\mathbf{t}}_i^T\}\right]^T \in \mathbb{R}^{2F_sN\times 1},\\
\breve{\mathbf{P}}_i{}^R &= \begin{bmatrix} \mathrm{Re}\{\breve{\mathbf{P}}_\mathrm{i}\} & -\mathrm{Im}\{\breve{\mathbf{P}}_\mathrm{i}\} \\ \mathrm{Im}\{\breve{\mathbf{P}}_\mathrm{i}\} & \mathrm{Re}\{\breve{\mathbf{P}}_\mathrm{i}\} \end{bmatrix} \in \mathbb{R}^{2F_sN\times 2(N-K)},\\
\mathbf{u}_i^R &= \left[\mathrm{Re}\{\mathbf{u}_i^T\} \quad \mathrm{Im}\{\mathbf{u}_i^T\}\right]^T \in \mathbb{R}^{2(N-K)\times 1},\\
\breve{\mathbf{Q}}_i{}^R &= \begin{bmatrix} \mathrm{Re}\{\breve{\mathbf{Q}}_\mathrm{i}\} & -\mathrm{Im}\{\breve{\mathbf{Q}}_\mathrm{i}\} \\ \mathrm{Im}\{\breve{\mathbf{Q}}_\mathrm{i}\} & \mathrm{Re}\{\breve{\mathbf{Q}}_\mathrm{i}\} \end{bmatrix} \in \mathbb{R}^{2N\times 2(N-K)}.
\end{aligned}$$

Then, we have

$$\begin{aligned}
&\min_{\mathbf{u}_i} \left\|\breve{\mathbf{t}}_i^R + \breve{\mathbf{P}}_i{}^R\mathbf{u}_i^R\right\|_\infty \\
&\text{subject to } \left\|\breve{\mathbf{Q}}_i^R\mathbf{u}_i^R\right\|_\infty \le \beta_1,\ \left\|\breve{\mathbf{P}}_i{}^R\mathbf{u}_i^R\right\|_2 \le \sqrt{\alpha}\left\|\breve{\mathbf{t}}_i^R\right\|_2.
\end{aligned} \tag{13}$$

Introducing an auxiliary variable τ, the problem (13) can be equivalently written as

$$\begin{aligned}
&\min_{\mathbf{u}_i,\tau} \tau \\
&\text{subject to } -\tau\cdot\mathbf{1} \le \breve{\mathbf{t}}_i^R + \breve{\mathbf{P}}_i{}^R\mathbf{u}_i^R \le \tau\mathbf{1}, \\
&-\sqrt{\frac{\beta_1^2}{2}}\cdot\mathbf{1} \le \breve{\mathbf{Q}}_i^R\mathbf{u}_i^R \le \sqrt{\frac{\beta_1^2}{2}}\cdot\mathbf{1},\ \left\|\breve{\mathbf{P}}_i{}^R\mathbf{u}_i^R\right\|_2 \le \sqrt{\alpha}\left\|\breve{\mathbf{t}}_i^R\right\|_2
\end{aligned} \tag{14}$$

where the first and second constraints hold for each component. The first and second constraints in (14) can be simplified respectively as

$$\mathbf{A}_i^R\boldsymbol{\omega}_i \le \mathbf{b}_i^R \tag{15}$$

$$\mathbf{Q}_i^R\boldsymbol{\omega}_i \le \sqrt{\frac{\beta_1^2}{2}}\cdot\mathbf{1}_{4N} \tag{16}$$

where $\mathbf{A}_i^R \in \mathbb{R}^{4F_sN\times\{2(N-K)+1\}}$, $\boldsymbol{\omega}_i \in \mathbb{R}^{\{2(N-K)+1\}\times 1}$, $\mathbf{Q}_i^R \in \mathbb{R}^{4N\times\{2(N-K)+1\}}$, and $\mathbf{b}_i^R \in \mathbb{R}^{4F_sN\times 1}$ are defined as

$$\mathbf{A}_i^R = \begin{bmatrix} -\breve{\mathbf{P}}_i{}^R & -\mathbf{1}_{2F_sN} \\ \breve{\mathbf{P}}_i{}^R & -\mathbf{1}_{2F_sN} \end{bmatrix}, \boldsymbol{\omega}_i = \begin{bmatrix} \mathbf{u}_i^R \\ \tau \end{bmatrix},$$

$$\mathbf{Q}_i^R = \begin{bmatrix} \breve{\mathbf{Q}}_i{}^R & \mathbf{0}_{2N} \\ -\breve{\mathbf{Q}}_i{}^R & \mathbf{0}_{2N} \end{bmatrix}, \mathbf{b}_i^R = \begin{bmatrix} \breve{\mathbf{t}}_i^R \\ -\breve{\mathbf{t}}_i^R \end{bmatrix}.$$

Combining (16) and (16), we have

$$\boldsymbol{\Lambda}_i\boldsymbol{\omega}_i \le \mathbf{b}_i \tag{17}$$

where $\boldsymbol{\Lambda}_i \in \mathbb{R}^{\{4F_sN+4N\}\times\{2(N-K)+1\}}$ and $\mathbf{b}_i \in \mathbb{R}^{\{4F_sN+4N\}\times 1}$ are defined as follows.

$$\boldsymbol{\Lambda}_i = \begin{bmatrix} \mathbf{A}_i^R \\ \mathbf{Q}_i^R \end{bmatrix},\ \mathbf{b}_i = \begin{bmatrix} \mathbf{b}_i^R \\ \sqrt{\frac{\beta_1^2}{2}}\cdot\mathbf{1}_{4N} \end{bmatrix}.$$

Using the variable $\boldsymbol{\omega}_i$, we can simplify the third constraint in (14) as

$$\left\|\boldsymbol{\Psi}_i\boldsymbol{\omega}_i\right\|_2 \le \epsilon_i \tag{18}$$

TABLE I
SIMULATION PARAMETERS.

Modulation scheme	16QAM
Number of subcarriers N	128
Number of subcarriers per sub-block n	4
Number of active subcarriers per sub-block k	2
Number of sub-blocks g	32
A total of number of active subcarriers K	64
CP length N_p	32
Channel order L_h	10
Oversampling factor F_s	4
Minimum value of transmission symbol size σ	$\sqrt{2}$
Amplitude upper limit of proposed method β	0.4
Power limit parameter α	0.2
SSPA parameter ρ	2
SNR	40dB

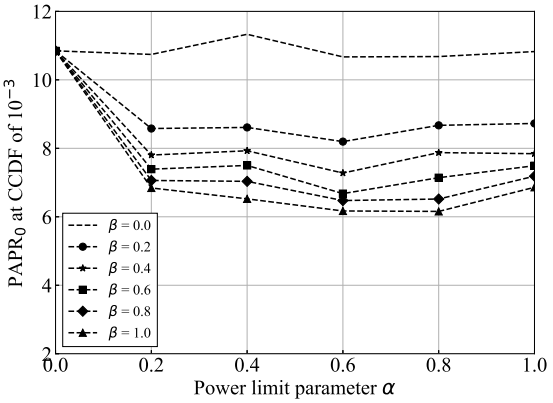

Fig. 3. Effect of α on PAPR performance.

where $\epsilon_i = \sqrt{\alpha}\|\breve{\mathbf{t}}_i^R\|_2$ and $\boldsymbol{\Psi}_i \in \mathbb{R}^{2N\times\{2(N-K)+1\}}$ is given by

$$\boldsymbol{\Psi}_i = \left[\breve{\mathbf{P}}_i{}^R \quad \mathbf{0}_{2N}\right].$$

Finally, we have the following optimization problem:

$$\begin{aligned}
&\min_{\boldsymbol{\omega}_i} \mathbf{e}^T\boldsymbol{\omega}_i, \\
&\text{subject to } \boldsymbol{\Lambda}_i\boldsymbol{\omega}_i \le \mathbf{b}_i,\ \left\|\boldsymbol{\Psi}_i\boldsymbol{\omega}_i\right\|_2 \le \epsilon_i
\end{aligned} \tag{19}$$

where $\mathbf{e} = [\mathbf{0}_{2(N-K)}\ 1]^T \in \mathbb{R}^{\{2(N-K)+1\}\times 1}$. The problem (19) can be solved using the interior point method for second-order cone programming (SOCP) problems. For this purpose, we can use a convex optimization solver such as CVXOPT [11].

IV. Simulation Results

Through computer simulations, we evaluate PAPR and BER performance of the proposed method, and compare with the conventional method in [6] and the original OFDM-IM. Unless otherwise stated, we used the parameters in Table I.

The effects of α on PAPR and BER performances for various β are shown in Figs. 3 and 4. The vertical axis represents the PAPR that achieves complementary cumulative distribution functions (CCDF) of 10^{-3}, i.e., PAPR_0 of $\Pr(\mathrm{PAPR} > \mathrm{PAPR}_0) = 10^{-3}$. Note that the performance of $\beta = 0.0$ corresponds to

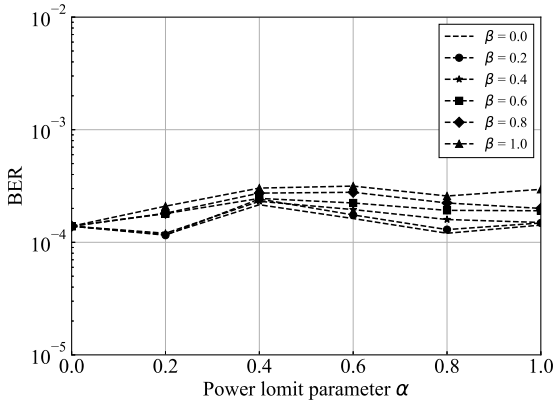

Fig. 4. Effect of α on BER performance.

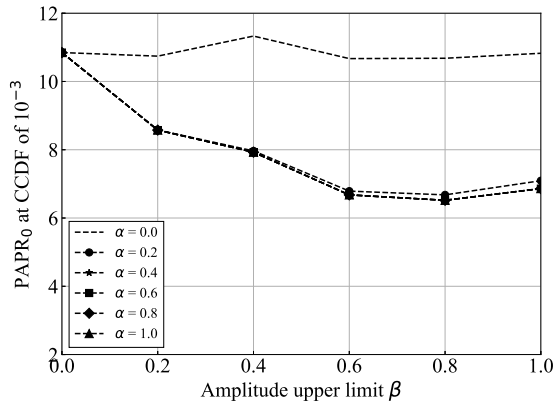

Fig. 5. Effect of β on PAPR performance.

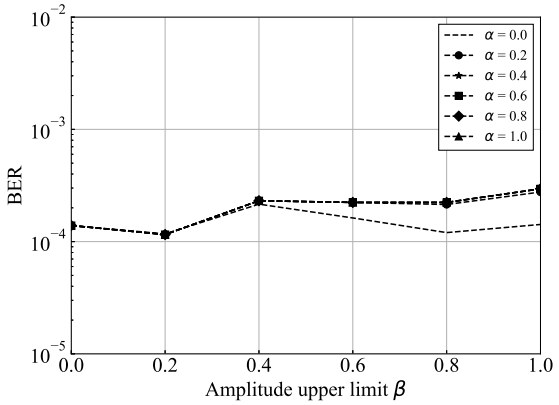

Fig. 6. Effect of β on BER performance.

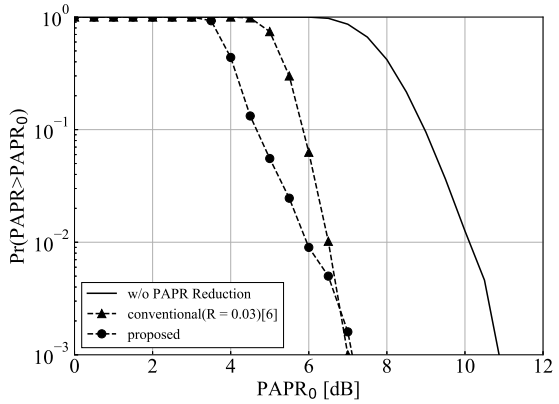

Fig. 7. PAPR performance when QPSK is employed.

the original OFDM-IM since a dither signal becomes zero. As α increases from 0 to 0.2, PAPR decreases, and BER becomes worse. When $\beta = 1.0$, PAPR is reduced by 4dB compared to the original OFDM-IM($\beta = 0$), but BER is slightly worse.

In Figs. 5 and 6, the effects of β on PAPR and BER performances for various α are shown. Note that the performances of $\alpha = 0.0$ correspond to the original OFDM-IM. As β increases, PAPR decreases, and BER becomes worse. When $\beta \leq 0.4$, BER of the proposed method is almost the same as that of the original OFDM-IM. From these results, we use $\alpha = 0.2$ and $\beta = 0.4$ in the following simulations.

Figs. 7 and 8 show the comparison of PAPR performance of various methods for QPSK and 16QAM, respectively. The magnitude limitation level R of the conventional method [6] is determined such that the PAPR_0 of 10^{-3} of the proposed method is almost the same as that of the conventional method, R =0.03 for QPSK and 0.075 for 16QAM. The performance of 16QAM is worse than that of QPSK. The proposed method can reduce PARP more than 3dB compared to the original OFDM-IM at CCDF of 10^{-3}.

In Figs. 9 and 10, the comparison of BER performance of various methods over Rayleigh fading channel for QPSK and 16QAM, respectively. The performance of the conventional method [6] is significantly degraded due to the misdetection of active subcarriers at the receiver. We can observe that BER of the proposed method is almost the same as that of the original OFDM-IM.

Figs. 11 and 12 show the power spectrum density (PSD) of the original OFDM-IM and the proposed method. We use a solid state power amplifier (SSPA) whose AM/AM characteristic is $g(x) = x(1+(x/x_{sat})^{2\rho})^{-1/2\rho}$ where x_{sat} is the saturation level and ρ controls the AM/AM sharpness of the saturation region, and input back off (IBO) is 0, 3, and 7dB. When IBO = 0 and 3dB, the PSD of the proposed method is about 5dB lower than the original OFDM-IM at the frequency of 5 MHz. When IBO = 7dB, the proposed method provides almost the same PSD as the case with a linear amplifier.

V. Conclusions

In this paper, we proposed a PAPR reduction method using a dither signal for OFDM-IM. By using the channel knowledge at the transmitter, the dither signal is determined so as not only to reduce PAPR at the transmitter but also to avoid the misdetection of active subcarriers at the receiver. Simulation results showed that the BER performance of the proposed method is superior to a conventional method and the PAPR performance of the proposed method is better than the original OFDM-IM.

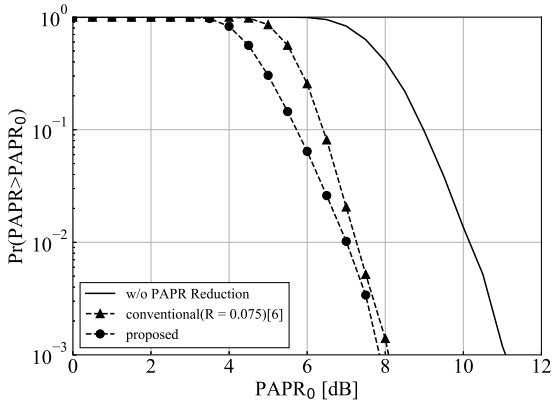

Fig. 8. PAPR performance when 16QAM is employed.

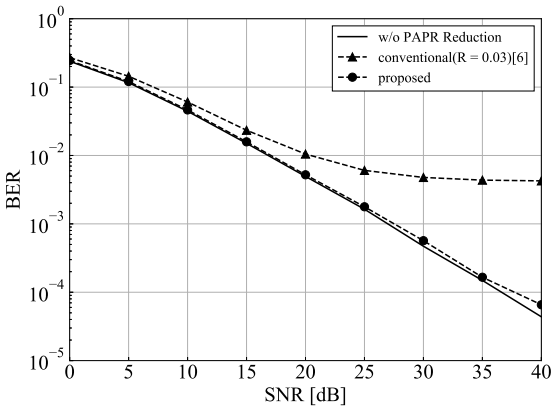

Fig. 9. BER performance when QPSK is employed.

REFERENCES

[1] E. Basar, "Index modulation techniques for 5G wireless networks," *IEEE Commun. Mag.,* vol. 54, no. 7, pp. 168–175, July 2016.
[2] T. Mao, Q. Wang, Z. Wang, and S. Chen, "Novel index modulation techniques: a survey," *IEEE Commun. Surveys Tuts.,* vol. 21, no. 1, pp. 315–348, 1th Quart 2019.
[3] E. Basar, Ü. Aygölü, E. Panayirci, and H. V. Poor, "Orthogonal frequency division multiplexing with index modulation," *IEEE Trans. Signal Process.,* vol. 61, no. 22, pp. 5536–5549, Nov. 2013.
[4] N. Ishikawa, S. Sugiura, and L. Hanzo, "Subcarrier-index modulation aided OFDM-will it work?," *IEEE Access,* vol. 4, pp. 2580–2593, 2016.
[5] Y. Rahmatallah and S. Mohan, "Peak-to-average power ratio reduction in OFDM systems: a survey and taxonomy," *IEEE Commun. Surveys Tuts.,* vol. 15, no. 4, pp. 1567–1592, 4th Quart 2013.
[6] J. Zheng and H. Lv, "Peak-to-average power ratio reduction in OFDM index modulation through convex programming," *IEEE Commun. Lett.,* vol. 21, no. 37 pp. 1505–1508, July 2017.
[7] K. H. Kim, "PAPR reduction in OFDM-IM using multilevel dither signals," *IEEE Commun. Lett.,* vol. 23, no. 2 pp. 258–261, Feb. 2019.
[8] E. Memisoglu, E. Basar, and H. Arslan, "Low complexity peak-to-average power ratio reduction in OFDM-IM," *Proc. 2018 IEEE Int. Black Sea Conf. Commun. Netw.,* pp. 1–5, Jun. 2018.
[9] J. Crawford and Y. Ko, "Low complexity greedy detection method with generalized multicarrier index keying OFDM," *Proc. 2015 IEEE PIMRC*, pp. 688–693, Aug. 2015.
[10] Z. E. Ankarali, A. Sahin, and H. Arslan, "Joint time-frequency alignment for PAPR and OOBE suppression of OFDM-based waveforms," *IEEE Commun. Lett.,* vol. 21, no. 12 pp. 2586–2589, Dec. 2017.
[11] M. S. Andersen, J. Dahl and L. Vandenberghe, CVXOPT documentation release 1.2.1. https://media.readthedocs.org/pdf/cvxopt/dev/cvxopt.pdf, pp. 1-135, Aug. 2018.

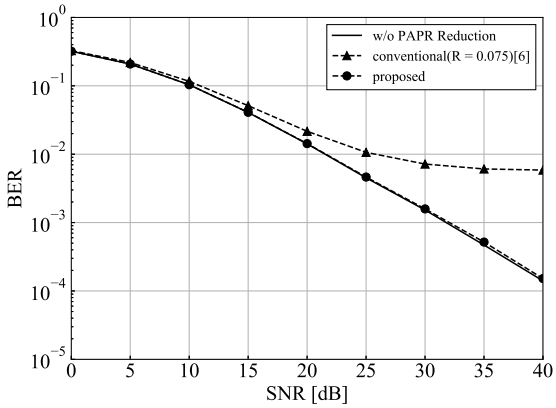

Fig. 10. BER performance when 16QAM is employed.

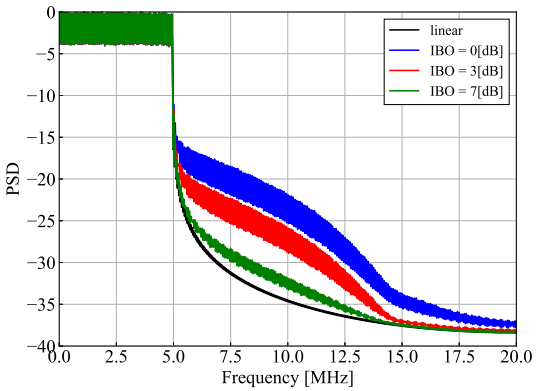

Fig. 11. PSD performance (original OFDM-IM).

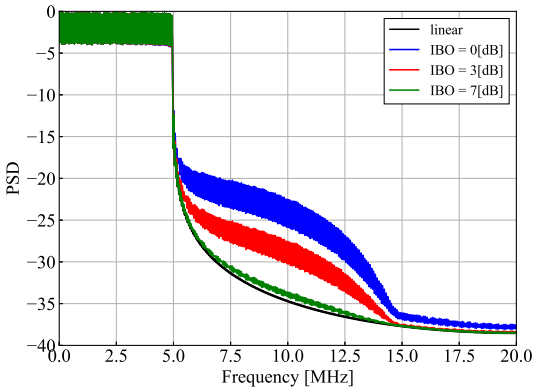

Fig. 12. PSD performance (proposed).